EDGEWOOD
CHEMICAL BIOLOGICAL CENTER
U.S. ARMY SOLDIER AND BIOLOGICAL CHEMICAL COMMAND

ECBC-TR-084

CHARACTERIZATION AND INTERPRETATION OF SPECTRA FROM A DUAL-BEAM FT-IR INTERFEROMETER USING A HEATED GAS CELL

Ronald E. Shaffer

NAVAL RESEARCH LABORATORY
Washington, DC 20375-5342

Roger J. Combs

RESEARCH AND TECHNOLOGY DIRECTORATE

May 2000

Aberdeen Proving Ground, MD 21010-5424

Disclaimer

The findings in this report are not to be construed as an official Department of the Army position unless so designated by other authorizing documents.

REPORT DOCUMENTATION PAGE

Form Approved
OMB No. 0704-0188

1. AGENCY USE ONLY *(Leave Blank)*	2. REPORT DATE	3. REPORT TYPE AND DATES COVERED
	May 2000	Final; Jan 99 - Jun 99

4. TITLE AND SUBTITLE
Characterization and Interpretation of Spectra from a Dual-beam FT-IR Interferometer Using a Heated Gas Cell

5. FUNDING NUMBERS
PR-20140/CB2

6. AUTHOR(S)
Shaffer, Ronald E. (NRL) and Combs, Roger J. (ECBC)

7. PERFORMING ORGANIZATION NAME(S) AND ADDRESS(ES)
Naval Research Laboratory, ATTN: Code 6116, Washington DC 20375-5342
DIR, ECBC, ATTN: AMSSB-RRT-DI, APG, MD 21010-5424

8. PERFORMING ORGANIZATION REPORT NUMBER
ECBC-TR-084

9. SPONSORING/MONITORING AGENCY NAME(S) AND ADDRESS(ES)

10. SPONSORING/MONITORING AGENCY REPORT NUMBER

11. SUPPLEMENTARY NOTES

12a. DISTRIBUTION/AVAILABILITY STATEMENT
Approved for public release; distribution is unlimited

12b. DISTRIBUTION CODE

13. ABSTRACT *(Maximum 200 words)*

The commercially available model MR254/AB FT-IR spectrometer is based on a dual-beam interferometer design. One arm of the dual-beam interferometer uses an internally controlled blackbody source for passive standoff airborne applications. This configuration with an internal blackbody produces a variety of output spectra that do not necessarily follow the output spectral conventions of a single-beam FT-IR spectrometer. The differences between a dual-beam and single-beam instrument are documented with eight examples using the radiance equation that models the dual-port MR254/AB spectrometer spectral response in terms of internal blackbody, gas cell, and background blackbody spectroradiometric temperatures.

14. SUBJECT TERMS
Dual-beam interferometer
Passive FT-IR Spectrometry
Heated Vapor/Gas Cell

15. NUMBER OF PAGES
24

16. PRICE CODE

17. SECURITY CLASSIFICATION OF REPORT	18. SECURITY CLASSIFICATION OF THIS PAGE	19. SECURITY CLASSIFICATION OF ABSTRACT	20. LIMITATION OF ABSTRACT
UNCLASSIFIED	**UNCLASSIFIED**	**UNCLASSIFIED**	**UL**

Blank

PREFACE

This work described in this report was authorized under Project No. 20140/CB2, Safeguard. The work started in January 99 and completed in June 99.

The use of either trade or manufacturers' names in this report does not constitute an official endorsement of any commercial products. This report may not be cited for purposes of advertisement.

This report has been approved for public release. Registered users should request additional copies from the Defense Technical Information Center; unregistered users should direct such requests to the National Technical Information Service.

Blank

CONTENTS

FIGURES

TABLES

Characterization and Interpretation of Spectra from a Dual-Beam FT-IR Interferometer Using a Heated Gas Cell

1. INTRODUCTION

Airborne passive detection of chemical vapors has been demonstrated using a commercially available Fourier transform infrared (FT-IR) spectrometer made by Bomem, Inc. (Quebec, CANADA). The Bomem MR254/AB FTIR spectrometer features a unique double-beam interferometer design that offers great potential to improve sensitivity and radiometric stability. However, the interferogram-based data analysis methodology developed during collaborative research efforts between Ohio University (Athens, Ohio) and the U.S. Army ECBC has been focused on conventional single-beam interferometer designs. In the work considered in this report, radiometric models are developed to describe the unique interferometer design and to assess how this design impacts current data analysis protocols. To meet this objective, interferograms are collected while a heated gas cell and a temperature controlled infrared blackbody source serving as a background are in the field of view of the spectrometer. The gas cell is quantitatively filled with known chemical vapors and heated to target temperatures to simulate passive airborne measurement conditions. Ethanol is the target gas. Nitrogen and sulfur dioxide serve as the background and interfering chemical vapors, respectively. Characterization and interpretation of these spectra is performed to gain insight into the influence of radiometric parameters upon signal quality.

2. EXPERIMENTAL PROCEDURES

The data used in this report were collected by Aerosurvey, Inc. under Army Contract Number DAAD05-98-P-1806.[1] Certified reference gases of ethanol and sulfur dioxide (8 different concentrations) were studied under nine gas cell temperatures and eight background blackbody temperatures. For each set of sample conditions, 128 or more replicate interferograms were collected. Further experimental details were documented in the Aerosurvey, Inc. report.

For each set of sample conditions, a data file containing replicate interferograms was generated. A total of 576 files (9 gas temperatures $\times$ 8 concentrations $\times$ 8 blackbody temperatures = 576) were acquired with ethanol present in the gas cell. For each experiment with ethanol in the cell, an analogous experiment was performed with the gas cell filled with nitrogen (i.e., blank cell). These interferograms served as the background files for purposes of computing absorbance spectra since nitrogen gas was not infrared active. A set of 128 files (2 gas temperatures $\times$ 8 concentrations $\times$ 8 blackbody temperatures) were collected while sulfur dioxide was present in the gas cell and another 128 under the same conditions with only nitrogen present. Other files were taken with TEP and ethylene in the gas cell but were not considered in this work.

These gases had another 79 background files associated with them. In addition to the experiments with a gas cell, another set of 16 experiments were conducted while the gas cell was not in the field of the view of the spectrometer. In this work, only the interferograms obtained at 16 cm^{-1} spectral resolution were used. Data from experiments using higher spectral resolutions (8, 4, 2, and 1 cm^{-1}) were removed from further analysis. Thus, interferograms from a total of 1504 experiments were available for this study. However, several files listed in the Aerosurvey report were missing on the disks received by the author (RES) and assumed to have been lost during the transfer to computer. A thorough outlier analysis was performed to remove any files that had been mislabeled. Background files labeled *enea2* and *enda5* were found to contain significant ethanol infrared absorbance features while *enha* appears to have been collected at a different background temperature than reported. Table 1 lists the makeup of the data files used in this study.

Table 1. Heated Gas Cell Data Set

Experiment	**Number of Files**
Ethanol	575
Background	567
Sulfur Dioxide	128
Background	128
Other backgrounds	79
Blackbody only (no gas cell)	16
Total	**1491**

3. RADIOMETRIC MODEL FOR THE BOMEM MR254/AB DUAL-BEAM INTERFEROMETER

The Bomem MR254/AB FTIR spectrometer utilizes a unique double-beam interferometer design as shown in Figure 1. In this design, the two input radiances are optically subtracted from each other at the beamsplitter.[2-5] This differs greatly from the single-beam design used in many commercial FTIR spectrometers. The Bomem design was conceived so that one of the inputs views the gas while the other would be aligned with an appropriate adjacent background. The two scene radiances are optically subtracted from each other prior to reaching the detector, thereby eliminating most features associated with the adjacent background. Using this "differential detection procedure", Theriault and coworkers have shown great sensitivity in detecting and quantifying gas plumes in controlled outdoor experiments.[3-5]

For airborne measurements from a moving platform, this approach is not viable, since a "true" background can not be definitively determined during

the course of a mission. The differential detection method works best only when the two ports view adjacent scenes (one with the gas and one without the gas present) where the background radiance levels are similar. When these conditions are not met, the optical subtraction often leaves large residual background features. The analysis is further complicated for real-time airborne measurements since the second port is not easily moved in the direction of a desirable background. For these reasons, airborne applications should use a modified spectrometer in which input port #2 is blocked with a controlled blackbody infrared source. The temperature of the "internal" blackbody is designed to coincide with the temperature of the spectrometer. Thus, each the energy seen at the detector is a function of the radiance from the scene coming from input port #1, E_1, and the internal blackbody sitting in front of input port #2, E_2.

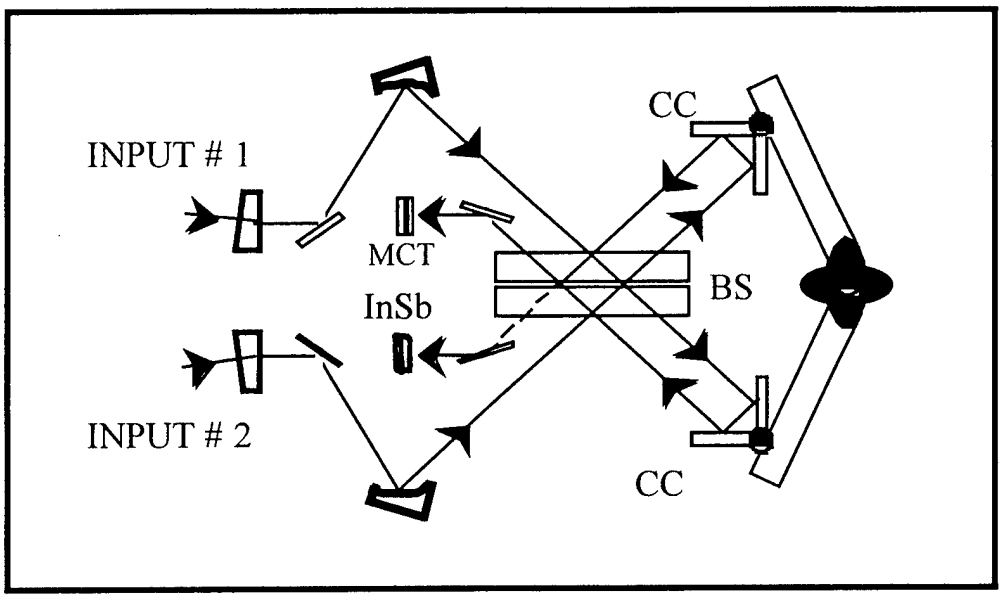

Figure 1. Schematic of the Dual-Beam Interferometer Design Used in the Bomem MR254/AB Spectrometer.

To understand how each of the radiation sources affect the interferogram (or single-beam spectrum), radiometric models were developed.[6-9] A single-beam spectrum obtained from a conventional interferometer design with a single input port can be expressed mathematically as

$$S = \Re(L_x + L_e) \quad (1)$$

where $\Re$ is the FT-IR instrument responsivity or gain, L_e is the FT-IR instrument self-emission function or offset, L_x is the radiance coming from the input port (i.e., the field of view of the FT-IR), and S is the measured single-beam spectrum. The instrument offset term arises from the combination of emission and

scattering contributions of various components of the optical train. The instrument responsivity, sometimes called the instrument response function, is a measure of the sensitivity of the detector at each infrared frequency.

The spectral radiance measured at the detector in a double input port interferometer design is the function of two radiances. This relationship can be expressed mathematically as

$$S = E_1 + E_2 \tag{2}$$

with

$$E1 = \Re_1 (L_{x1} + L_{e1}) \tag{3}$$

and

$$E2 = -\Re_2 (L_{x2} + L_{e2}) \tag{4}$$

where L_{x1} and L_{x2} are the radiances from the spectrometer field of view for each input port, $\Re_1$ and $\Re_2$ are the responsivities associated with each input port, and L_{e1} and L_{e2} are the self-emission profiles for each input. An optical subtraction is performed at the beamsplitter by having the two input paths (E_1 and E_2) 180° out of phase with each other. In a perfectly balanced, symmetric dual-beam interferometer design, ($\Re_1 = -\Re_2$) and ($L_{x1} = L_{x2}$). However, in a series of recently published papers, Theriault and coworkers have shown that residuals exist due to asymmetry in the beamsplitter.[2-5] Because the work here relies on the models only for interpretation and explanation of spectral artifacts, we will assume that a balanced symmetric interferometer exists. This allows us make use of these simplifications and to derive a simple radiometric model for the Bomem FT-IR spectrometer that is given in equation 5.

$$S = \Re (L_{x1} - L_{x2}) \tag{5}$$

The instrument responsivity term in equation 5 can be computed using the two temperature calibration scheme described by Revercomb and coworkers.[10] In the modified Bomem MR254/AB instrument, input port #2 has a temperature controlled blackbody infrared source.

4. RADIOMETRIC MODEL FOR HEATED GAS CELL DATA

To understand the contributions from the various radiometric sources in the heated gas cell data, a radiometric model is created. This model allows the generation of synthetic interferograms and spectra which can easily be broken down to each radiance source.

At a first level approximation, L_{x2} can be modeled as a Planck blackbody curve and equation 5 can be rewritten as

$$S = \Re\,(L_{x1} - L^{*}_{int}) \qquad (6)$$

where L^{*}_{int} represents the Planck radiance at the internal temperature (T_{int}) of the FT-IR spectrometer. In a previous report [9], Shaffer and Combs described a passive FT-IR radiometric model applicable for a single-port interferometer which can be adapted for use with the data from the heated gas cell,

$$L_x = [\tau_t\,\tau_a\,L_{bg} + (1 - \tau_t\,\tau_a)\,L_t] \qquad (7)$$

where τ_t is the transmittance of the analytes in the gas cell, τ_a is the transmittance of the atmosphere, L_{bg} is the radiance of the blackbody infrared background, L_t is the radiance of heated gas cell. The gas cell transmittance is defined as $\tau_t = \exp(-\alpha c l)$ where α is the absorptivity (m^2/mg) of the gas and c is the concentration of the gas (mg/m^3), and l is the optical pathlength (m) of the cell. This equation assumes that the gas cell fills the spectrometer field of view and negligible radiance losses occur due to scattering. For simplicity, it is assumed that L_{bg} and L_t are perfect blackbodies that are represented by Planck's function (L^{*}). These radiances depend solely on temperatures of the blackbody background (T_{bb}) and the gas cell (T_{gc}) respectively. It can also be assumed that the atmospheric transmission is negligible since the distance between the gas cell and the instrument was less than a few centimeters. Taking into account these assumptions and combining equations (6-7), we can produce a radiometric model for the heated gas cell data taken with the Bomem MR254/AB double-beam interferometer that is used in Program SAFEGUARD.

$$S = \Re\,([\tau_t\;L^{*}_{bb} + (1 - \tau_t)\,L^{*}_{gc}] - L^{*}_{int}) \qquad (8)$$

L^{*}_{gc} is the blackbody radiance of the heated gas cell contents. The quantity in the square brackets of equation 8 is the scene radiance.

5. SPECTRAL INTERPRETATION USING THE RADIOMETRIC MODEL

Four parameters (T_{int}, T_{bb}, T_{gc}, c) derived from the radiometric model given in equation 8 greatly effect the quality and interpretation of the single-beam spectra collected from the heated gas cell. Many of these effects are identical to the single-port interferometer case. For example, if $T_{bb} = T_{gc}$ then the τ_t terms cancel out and no analyte signature is seen in the resulting single-beam spectrum. Also, if the analyte concentration c drops below the limit of detection, the analyte signature cannot be discerned above the noise level. The importance of these two effects is discussed in great detail elsewhere.[6-9]

The difficulty in interpreting single-beam spectra from the Bomem MR254/AB instrument is caused by the radiances emitted from the internal

blackbody (L^*_{int}) which can be modeled by T_{int}. By itself, T_{int} has little effect on the resulting spectra. But when considered in conjunction with the temperatures of the gas cell (T_{gc}) and the blackbody background (T_{bb}), it plays a major role. In this report, we consider two special cases in which T_{bb} or T_{gc} are equal to T_{int}, as well as the more commonly encountered scenarios involving airborne or gas cell measurements. For radiometric model calculations, ethanol is used as the target analyte. Ethanol absorbance (and hence τ_t) is determined using Ballard's method[11] for computing an absorbance spectrum from FT-IR interferograms collected from a heated gas cell (i.e., target analyte) and an extended blackbody (i.e., background radiance). The ethanol concentration is set at 8000 ppm-m for all calculations, unless otherwise noted. In a previous report, the software (*ftir_toolbox*) for generating synthetic spectra and interferograms based on passive infrared radiometric models and a conventional single-input interferometer is described.[9] The software used here involves a modification of the code for incorporation of equation 8 into the calculations.

5.1 Equality of Background and Internal Temperatures ($T_{bb} = T_{int}$)

In the case of T_{bb} equals T_{int} equation 8 reduces to equation 9.

$$S = \Re [\tau_t (L^*_{bb} - L^*_{gc}) + (L^*_{gc} - L^*_{bb})] \quad (9)$$

The simplest way to understand the shape and profile of the single-beam spectra that would result from this situation is to plot E_1 and E_2 (i.e., L_{x1} and L^*_{int}) in spectral radiance units. Figure 2 shows plots of (A) E_1 and E_2 for the case where T_{int} = 50 °C, T_{bb} = 50 °C, and T_{gc} = 30 °C, (B) E_1 and E_2 for the case where T_{int} = 50 °C, T_{bb} = 50 °C, and T_{gc} = 160 °C, and (C) the resulting single-beam spectra 30 °C (lower trace) and 160 °C (upper trace). These plots illustrate the difficulty in interpreting the gas cell data. The lower single-beam spectrum in Figure 2C was generated with the gas cell colder than the background, which would typically result in absorption features, yet produces a single-beam spectrum with apparent infrared emission bands. This anomaly occurs because E_2 has larger spectral radiance values than E_1 (see Figure 2A). Thus, when they are subtracted, negative spectral radiance values would be generated. The interferogram software automatically detects this situation and "flips" the interferogram in the positive direction, resulting in the appearance of "emission-like" (i.e., apparent emission) spectral features. It is important to note that the optical subtraction at the detector is actually performed in the time domain where the absorption and emission signals are simply 180° out of phase with each other. The validity of the radiometric model is checked by comparing the above analysis with single-beam spectral collected using the same target conditions (Figure 3). In this figure, the spectrum shown with lower trace was collected with T_{int} = 50 °C, T_{bb} = 50 °C, and T_{gc} = 30 °C, while spectrum plotted in the upper trace was obtained for T_{int} = 50 °C, T_{bb} = 50 °C, and T_{gc} = 160 °C (same conditions as Figure 2C). The difference between Figures 2C and 3 are probably due to a slight asymmetry in the interferometer or an inaccurately determined

internal blackbody temperature. Another important interpretation from equation 9 can be made. Although it appears from the single-beam spectra that when $T_{bb} = T_{int}$ the radiance from the blackbody background (L^*_{bb}) is simply eliminated, ΔT ($T_{bb} - T_{gc}$) still plays a major role in determining the intensity of the bands. This point is illustrated in Figure 4 that shows three simulated single-beam spectra at $T_{bb} = T_{int} = 10$ °C (upper trace), $T_{bb} = T_{int} = 50$ °C (middle trace), and $T_{bb} = T_{int} = 90$ °C (bottom trace) with $T_{gc} = 160$ °C. As ΔT gets larger, the strength of the emission bands increase.

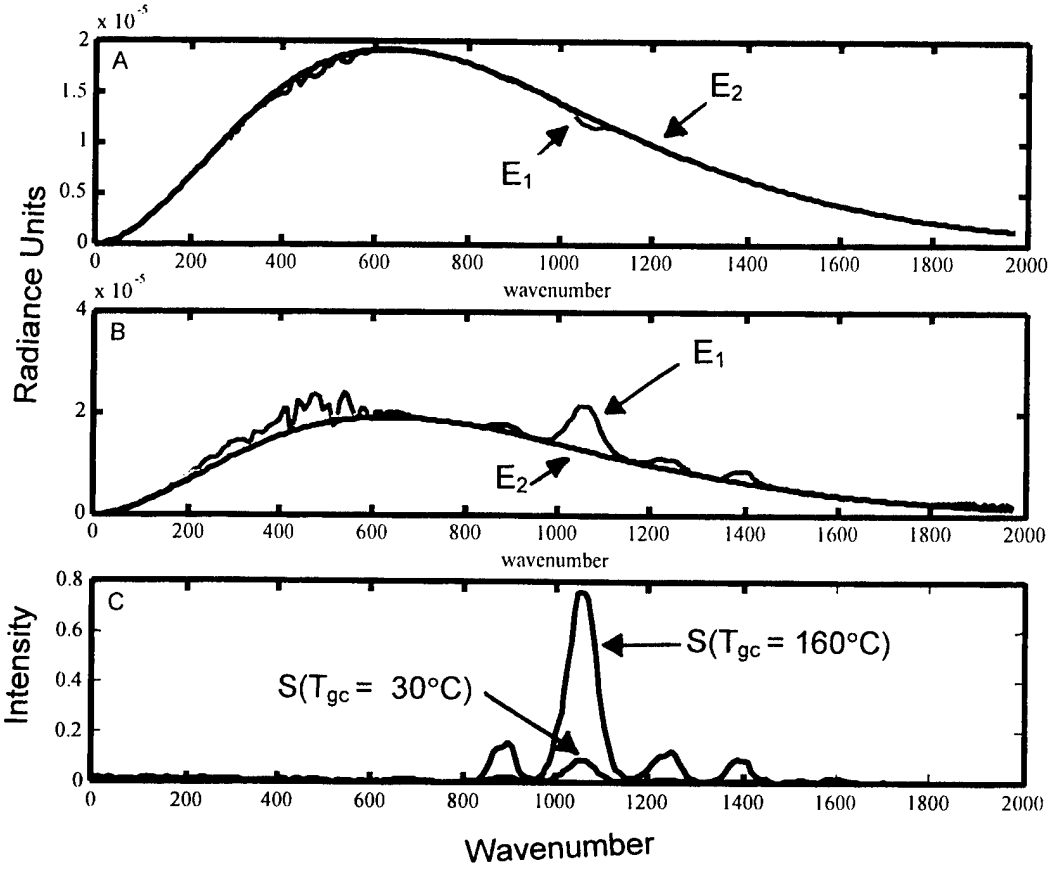

Figure 2. Equivalent Background and Internal Temperatures of 50 °C with gas cell temperatures of (A) 30 °C and (B) 160 °C. The resultant S spectra for absorption S(30 °C) and emission S(160 °C) are shown in (C).

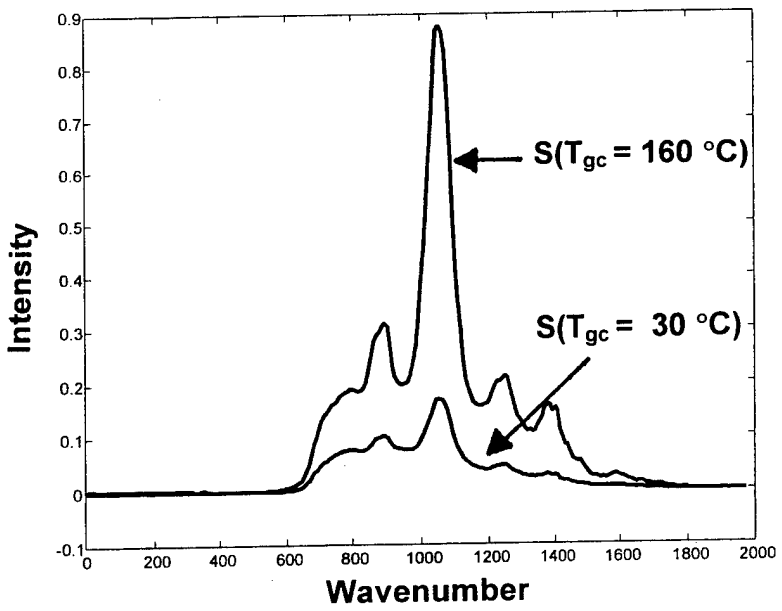

Figure 3. Residual Present in the Resultant S Spectra of S(30 °C) and S(160 °C). Same conditions as Figure 2C.

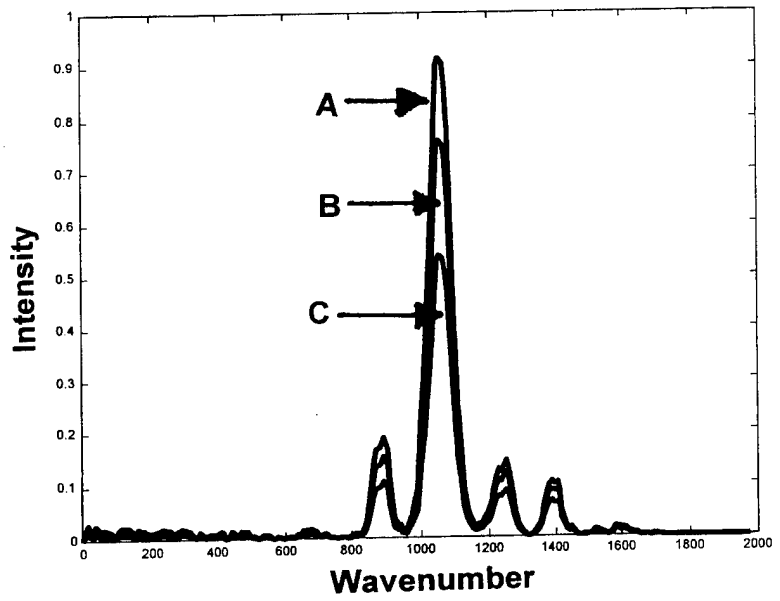

Figure 4. Effect on S Resultant Spectra of Internal and Background Radiometric Temperatures (i.e., $T_{bb} = T_{int}$) (A) 10 °C, (B) 50 °C, and (C) 90 °C for a constant gas cell temperature (i.e., T_{gc} = 160 °C).

5.2 Equality of Gas Cell and Internal Temperatures ($T_{gc} = T_{int}$)

In the case T_{gc} equals T_{int} equation 8 reduces to equation 10.

$$S = \Re [\tau_t (L^*_{bb} - L^*_{gc})] \quad (10)$$

This case offers an another example where the conventional rules concerning absorption and emission features (i.e., $T_{bb} > T_{gc}$ = absorption and $T_{bb} < T_{gc}$ = emission) cannot be used. In the case where the gas cell temperature equals the internal blackbody temperature, only absorption features can be found in the resultant single-beam spectra. This concept can be envisioned by studying E_1 and E_2 for two different situations. Figure 5 shows plots of (A) E_1 (lower trace) and E_2 (upper trace) for the case where T_{int} = 50 °C, T_{bb} = 10 °C, and T_{gc} = 50 °C, (B) E_1 (upper trace) and E_2 (lower trace) for the case where T_{int} = 50 °C, T_{bb} = 90 °C, and T_{gc} = 50 °C, and (C) the resulting single-beam spectra at background temperatures of 10 °C (lower trace) and 90 °C(upper trace). As these figures illustrate this situation is the opposite of that described in Section 5.1. The reason that absorption features are found in the situation where the gas cell is hotter than the background (see lower spectrum in Figure 5C) is similar to the explanation used earlier in the discussion of that in Section 5.1. In Figure 5A, E_1 the lower trace clearly shows an emission band (broad peak at 1066 cm^{-1} points upward), yet its overall radiance values are much smaller than that of the internal blackbody (E_2, upper trace). Thus, when E_2 is subtracted from E_1, negative values would be generated. The interferogram software automatically corrects for this situation, (i.e., the resultant spectrum is "flipped"), causing the emission feature to now have the appearance of an absorbance feature. This flip does not occur for the radiance spectra shown in Figure 5B because the subtraction results in positive values. Further interpretation of equation (10) indicates that ΔT ($T_{bb} - T_{gc}$) strongly influences band strength and the overall detector profile. This point is illustrated in Figure 6, which shows two resultant single-beam spectra collected while the heated gas cell of 8000 ppm-m ethanol was present in the field of view. In these spectra, the gas cell and internal blackbody temperature were both at approximately 49 °C ($T_{gc} \cong T_{int}$) while the external blackbody temperature was at 40 °C (lower trace) and 15 °C (upper trace). For a conventional interferometer, these spectra would show infrared emission since the gas cell temperature is hotter than the background, but because of the unique nature of the double-beam interferometer only absorption-like peaks are seen.

5.3 Equality of Gas Cell and Background Temperatures ($T_{gc} = T_{bb}$)

In the case of T_{gc} equals T_{bb} equation 8 reduces to equation 11.

$$S = \Re (L^*_{bb} - L^*_{int}) \quad (11)$$

This case follows the textbook single-beam interferometer example. When the

gas cell and background temperatures are equal no analyte signature is present (τ_t cancels out). The overall intensity of the single-beam spectra is dictated by the temperature difference between T_{gc} or T_{bb} and T_{int}.

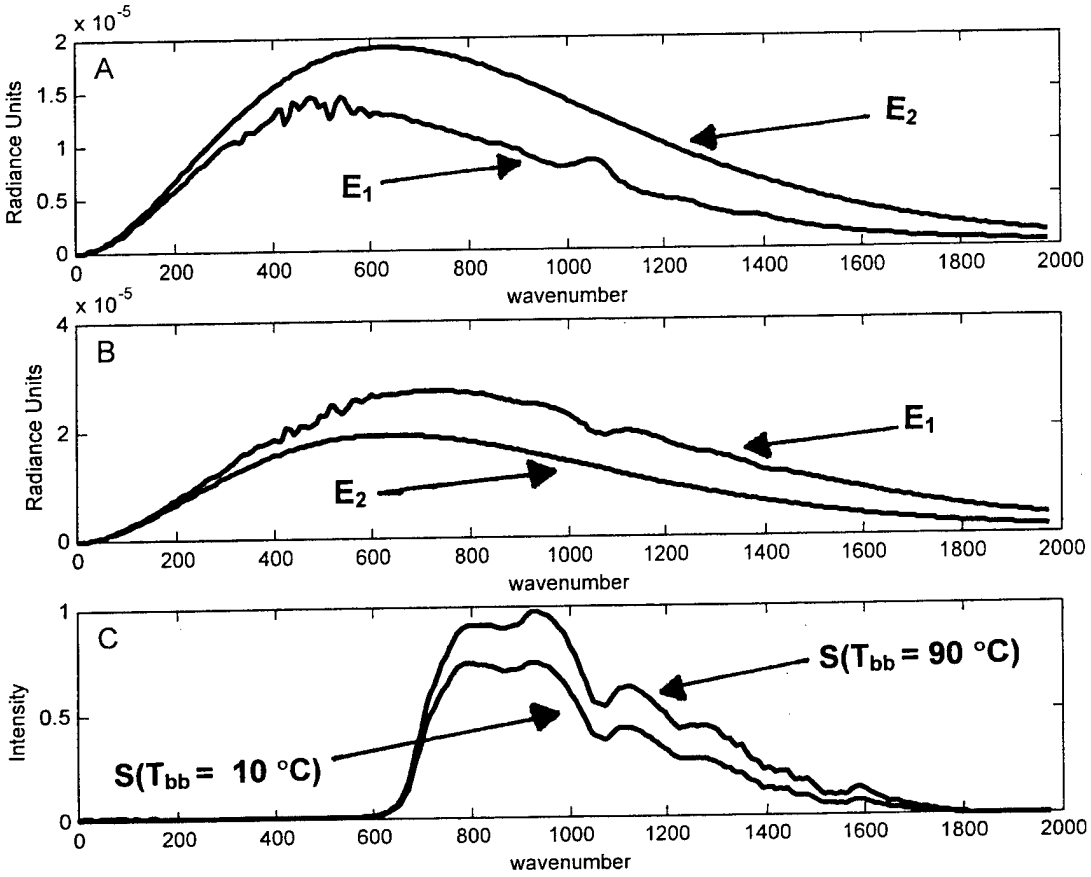

Figure 5. Equivalence of Gas Cell and Internal Radiance Temperatures of 50 °C with Background Temperatures of (A) 10 °C and (B) 90 °C. The resultant S spectra of $S(T_{bb} = 90\ °C)$ and $S(T_{bb} = 10\ °C)$ are shown in (C).

5.4 Equality of Gas Cell, Background, and Internal Temperatures ($T_{gc} = T_{bb} = T_{int}$)

Under these conditions, all the radiances terms in equation 8 cancel out. Thus, only a negligible signal is seen by the detector. An example of this is shown in Figure 7. In this plot, ethanol concentration was 8000 ppm-m, T_{gc} = 49.5 °C, T_{int} = 49 °C, and T_{bb} = 50 °C. Unfortunately, some residual is still left in the spectrum, but the overall single-beam intensity values are much smaller (by a factor of 50) than the other single-beam spectra in Figures 2C, 3, 4,

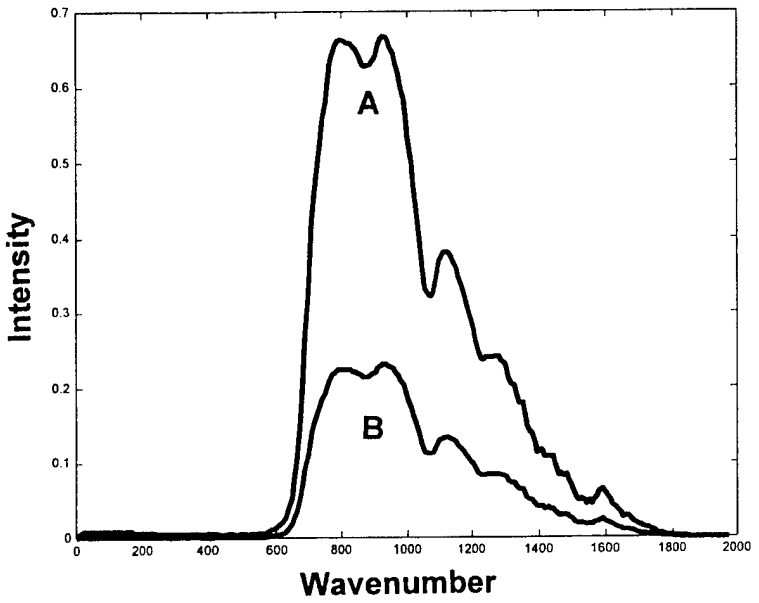

Figure 6. Equal Ethanol Cell and Internal Temperatures of 49 °C with Background Temperatures of (A) 45 °C and (B) 40 °C. Ethanol vapor concentration is 8000 ppm-m.

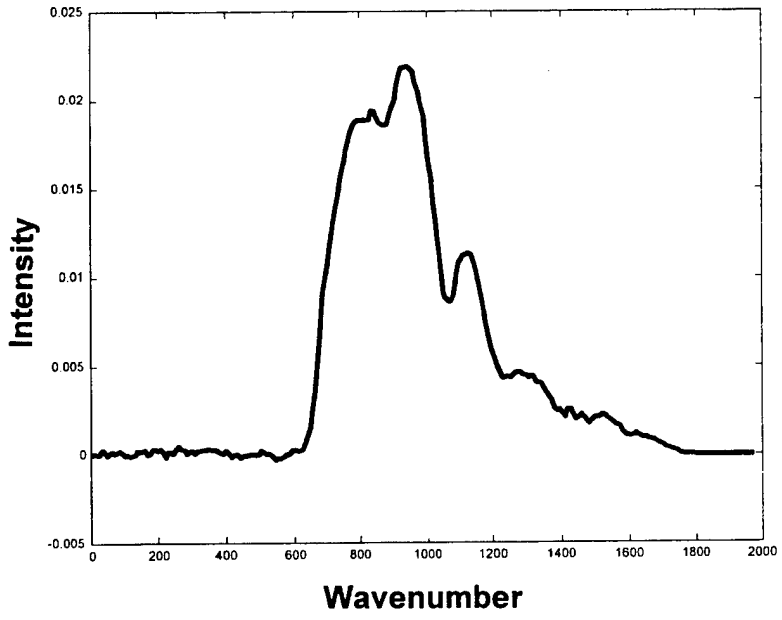

Figure 7. Residual Resultant S Spectrum for the Condition of $T_{gc} \cong T_{bb} \cong T_{int}$.

5C, and 6. The residual signal is due to the slight mismatch in temperatures and any self-emission radiances from the optics in the spectrometer.

5.5 Gas Cell and Background Temperatures greater than the Internal Temperature ($T_{int} < T_{gc}$ and T_{bb})

Given these conditions, the internal blackbody radiance (E_2) will always be less than the scene radiance (E_1). This scenario produces spectra like those collected on a single-input interferometer design and all conventional rules governing emission and absorbance apply. This occurs because E_1-E_2 will always produce positive values. Some example spectra are given in Figure 8. In this figure, the lower curve represents a synthetic spectrum of 8000 ppm-m ethanol in a gas cell at 90 °C with T_{int} = 10 °C and T_{bb} = 25 °C. The upper trace shows a synthetic spectrum of 8000 ppm-m ethanol in a gas cell at 25 °C with T_{int} = 10 °C and T_{bb} = 90 °C. As expected, the first spectrum exhibits emission features while the latter contains absorption bands.

5.6 Internal Temperature greater than Gas Cell and Background Temperatures ($T_{int} > T_{gc}$ and T_{bb})

Under these conditions, the internal blackbody radiance (E_2) will always be larger than the scene radiance (E_1). This scenario produces spectra that are opposite of those collected on a single-input interferometer design. The conventional wisdom regarding when emission and absorbance features will be present must be reversed. This reverse behavior occurs because E1-E2 will always produce negative values. Some example spectra are given in Figure 9. In this figure, the top trace represents a synthetic spectrum of 8000 ppm-m ethanol in a gas cell at 90 °C with T_{int} = 100 °C and T_{bb} = 10 °C. The bottom trace shows a synthetic spectrum of 8000 ppm-m ethanol in a gas cell at 10 °C with T_{int} = 100 °C and T_{bb} = 90 °C. As expected, the first spectrum exhibits absorption features while the latter contains emission bands.

5.7 Gas Cell Temperature greater than Internal Temperature greater than Background Temperature ($T_{gc} > T_{int} > T_{bb}$)

Under normal conditions this scenario produces spectra with similar qualities to those in Section 5.6. However, when T_{int} and T_{bb} have similar temperatures and the concentration of the gas is large a special case appears as shown in Figure 10. The Figure 10 spectra were generated using T_{gc} = 160 °C, T_{int} = 50 °C, T_{bb} = 10 °C and c = 8000 ppm-m. In Figure 10, E1 is larger than E2 at the emission bands of the analyte (1060 cm^{-1}). This causes the resulting S single-beam spectrum to have negative intensities, which are not physically possible in a conventional FT-IR spectrometer. If the concentration of the gas were smaller, then the emission band of E1 would still be smaller than E2 and

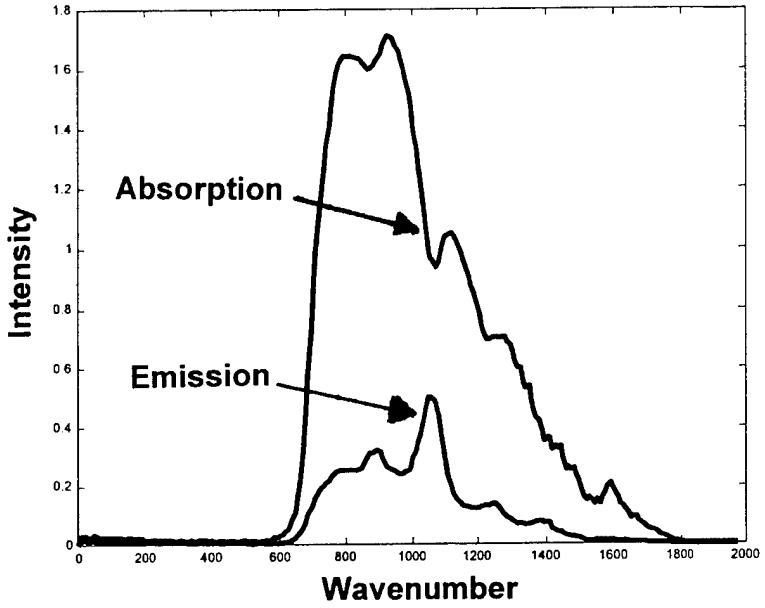

Figure 8. Response for Internal Temperature Lower Than Gas Cell and Background Temperatures. Spectral response similar to that encountered with a single-beam FT-IR spectrometer.

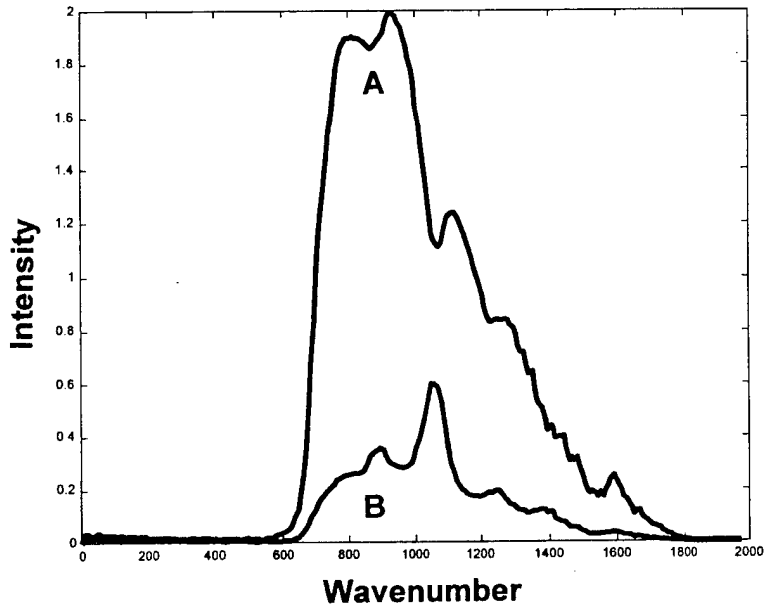

Figure 9. Response to Conditions of A ($T_{int} > T_{gc} > T_{bb}$) and B ($T_{int} > T_{bb} > T_{gc}$) are reverse of those encountered with a single-beam FT-IR spectrometer.

not negative bands would appear in the single-beam spectrum. If the temperature differential between T_{bb} and T_{int} were very large, it would be difficult to get the gas temperature hot enough or the concentration high enough to allow E1 to be more intense than E2. This scenario is very critical for for airborne scenarios because it is quite possible in the intended application to have very hot gas temperature (e.g., from a heated smoke stack) and a cold background (snow covered ground).

5.8 Gas Temperature less than Internal Temperature less than Background Temperature ($T_{gc} < T_{int} < T_{bb}$)

The final set of conditions occurs when the gas cell is colder and the background hotter than the internal temperature of the spectrometer. This situation will rarely be found in most remote sensing applications. If it does occur the spectra take on similar properties to those in Section 5.7. This can be illustrated using simulated spectra as shown in Figure 11. The spectra were created using T_{gc} = 10 °C, T_{int} = 50 °C, T_{bb} = 100 °C, and c = 40000 ppm-m. In Figure 11, E1 is smaller than the E2 at the absorbance bands of ethanol. Due to the optical subtraction, the resulting single-beam spectrum contains negative intensities where the analyte absorbs. This situation is difficult to create unless T_{gc} and T_{int} are very close or the analyte concentration large.

6. CONCLUSIONS

The resultant spectra IR signature for the Bomem MR254/AB, that is generated with a double-beam interferometer design, differs significantly from a traditional single-beam FT-IR spectrometer. The differences are described under a variety of conditions. These conditions are tabulated in Table 2. The target vapor of ethanol provides a spectral signature to assess whether the resultant spectrum appears as an apparent absorption or emission feature. The output of a conventional passive single-beam like spectra are obtained only for condition five, while an inversion of this type of output occurs for condition six. For conditions three and four, when the gas cell and background temperatures are nearly equal, a spectral signature is negligible or does not occur due to the low thermal contrast between sample and background. An apparent emission only results for condition one, while only an apparent absorption is discernable for condition two. Finally, negative apparent absorption features can arise for conditions seven and eight which are impossible for a single-beam interferometer design.

The responses of the Bomem MR254/AB dual-beam FT-IR spectrometer to a variety of laboratory conditions are documented. These responses provide guidance to modifications of single-beam FT-IR spectrometer signal processing methods needed to handle a dual-beam configuration. The types of spectral reponses for the dual-beam instrument are summarized by eight

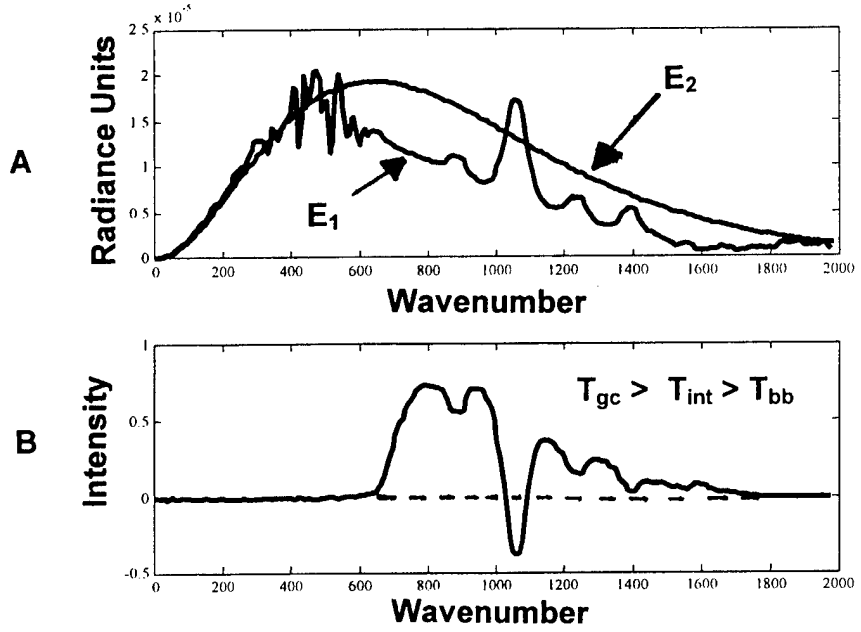

Figure 10. Response to Condition of $T_{gc} > T_{int} > T_{bb}$ for the two port radiances E_1 and E_2 are shown in A. The resultant S spectrum in B illustrates the negative going ethanol peak at 1060 cm^{-1} at 8000 ppm-m.

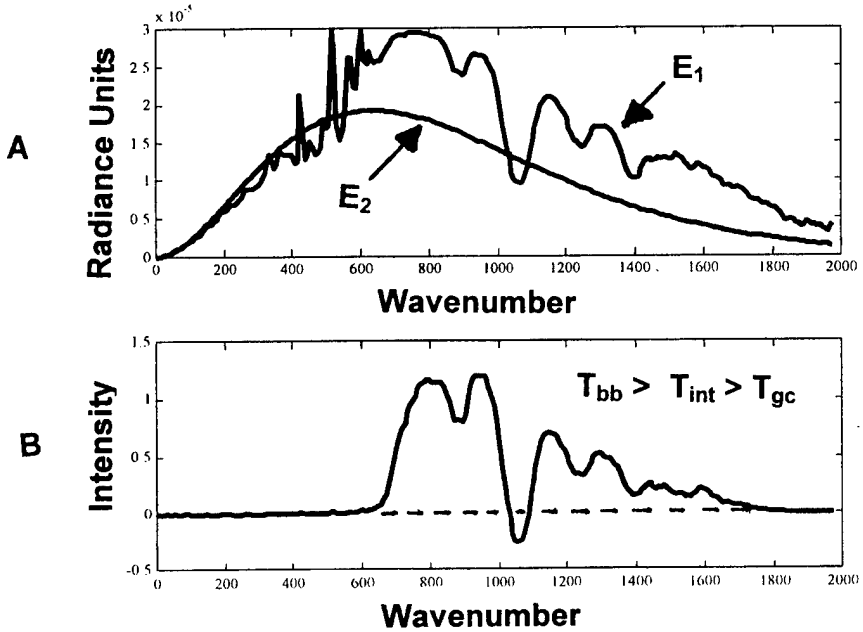

Figure 11. Response to Condition of $T_{bb} > T_{int} > T_{gc}$ for the two port radiances E_1 and E_2 are shown in A. The resultant S spectrum in B illustrates the negative going ethanol peak at 1060 cm^{-1} for 40000 ppm-m.

possible cases. The results indicate that proper selection of the internal temperature with either case five or six can simplify the signal processing strategy.

Table 2. Appearance of Ethanol Peaks for a Dual-beam FT-IR Spectrometer

Case	Condition	Ethanol Peak Appearance
1	$T_{gc} \neq T_{bb} = T_{int}$	Emission
2	$T_{bb} \neq T_{gc} = T_{int}$	Absorption
3	$T_{int} \neq T_{gc} = T_{bb}$	No Signature
4	$T_{int} = T_{gc} = T_{bb}$	No Signature[a]
5	$T_{gc} > T_{int}$, $T_{bb} > T_{int}$, $T_{gc} \neq T_{bb}$	Conventional
6	$T_{int} > T_{gc}$, $T_{int} > T_{bb}$, $T_{gc} \neq T_{bb}$	Opposite Conventional
7	$T_{gc} > T_{int} > T_{bb}$	Absorption[b]
8	$T_{bb} > T_{int} > T_{gc}$	Absorption[b]

[a]For example in Figure 7 only a residual spectrum of approximately zero.
[b]Negative going absorption peaks possible.

LITERATURE CITED

1. Chaffin, C.T. and Marshall, T.L. , "Laboratory Calibrations of Bomem MR254/AB," U.S. Army Contract # DAAD05-98-P-1806 with AeroSurvey, Inc., Aberdeen Proving Ground, MD, August 1998.

2. Villemaire, A.; Chamberland, M; Giroux, J.; Lachance, R.L.; and Theriault, J.-M., "Radiometric Calibration of FT-IR Remote Sensing Instrument," in *Electro-Optical Technology for Remote Chemical Detection and Identification II*, Fallahi, M. and Howden, E. eds., Vol. 3082, pp 83-91, SPIE, Bellingham, WA, 1997.

3. Theriault, J.-M.; Bradette, C.; Villemaire, A.; Chamberland, M.; and Giroux, J., "Differential Detection With a Double-beam Interferometer," in *Electro-Optical Technology for Remote Chemical Detection and Identification II*, Fallahi, M. and Howden, E. eds., Vol. 3082, pp 65-75, SPIE, Bellingham, WA, 1997.

4. Lachance, R.L.; Theriault, J.-M.; Lafond, C.; and Villemaire, A., "Gaseous Emanation Detection Algorithm Using a Fourier Transform Interferometer Operating in Differential Detection Mode," in *Electro-Optical Technology for Remote Chemical Detection and Identification III*, Fallahi, M. and Howden, E. eds., Vol. 3383, pp 124-132, SPIE, Bellingham, WA, 1998.

5. Theriault, J.-M., "Modeling the Responsivity and Self-Emission of a Double-Beam Fourier Transform Infrared Interferometer," *Applied Optics* Vol. 38, No. 3, pp 505-515 (1999).

6. Chaffin, C.T.; Marshall, T.L.; and Chaffin, N.C., "Passive FTIR Remote Sensing of Smokestack Emissions," *Field Analytical Chemistry and Technology* Vol. 3, No. 2, pp 111-115 (1999).

7. Combs, R.J., "Thermal Stability Evaluation for Passive FT-IR Spectrometry," *Field Analytical Chemistry and Technology* Vol. 3, No. 2, pp 81-94 (1999).

8. Flanigan, D.F., "Prediction of the Limits of Detection of Hazardous Vapors by Passive Infrared with Use of MODTRAN," *Applied Optics* Vol. 35, No. 30, pp 6090-6098 (1996).

9. Shaffer, R.E., and Combs, R.J., "Software for Generating Synthetic Passive Fourier Transform Infrared Interferograms and Single-Beam Spectra," NRL Memorandum Report 6110--92-8342, Naval Research Laboratory, Chemistry Division, Washington, DC, February 1999.

10. Revercomb, H.E.; Buijs, H.; Howell, H.B.; Laporte, D.D.; Smith, W.L.; and Sromovsky, L.A., "Radiometric Calibration of IR Fourier Transform Spectrometers: Solution to a Problem with the High-Resolution Interferometer Sounder," *Applied Optics* Vol. 27, No. 15, pp 3210-3218 (1988).

11. Ballard, J.; Remedios, J.J.; and Roscoe, H.K., "The Effect of Sample Emission on Measurement of Spectral Parameters Using a Fourier Transform Absorption Spectrometer," *Journal of Quantitative Spectroscopy and Radiative Transfer* Vol. 48, No. 316, pp 733-741 (1992).